



ELSEVIER

13 September 1999

PHYSICS LETTERS A

Physics Letters A 260 (1999) 286–293

www.elsevier.nl/locate/physleta

Local Larmor clock approach to the escape time

J.A. López Villanueva^a, V. Gasparian^{b,*}

^a *Departamento de Electrónica y Tecnología de Computadores, Campus de Fuentenueva, Universidad de Granada, Granada, Spain*

^b *Facultad de Química, Universidad de Guanajuato, Noria Alta s/n, Guanajuato, GTO. 36050, Mexico*

Received 16 May 1999; accepted 10 June 1999

Communicated by L.J. Sham

Abstract

The escape of an electron from a localized state in a quantum well with one or several surrounding barriers is analyzed using the local Larmor clock approach. We show that two time scales can be involved in the escape time problem, such as in the case of a scattering configuration. The particular example of a potential well with a hard wall condition on one side, i.e. escaping through only one open channel, is investigated, and the two time components are calculated analytically. One of the time components is shown to coincide with the lifetime expression obtained with a different approach, in the case of an opaque barrier, at an energy close to the bound level in the well. © 1999 Published by Elsevier Science B.V. All rights reserved.

1. Introduction

The calculation of the time interval during which a particle interacts with a barrier of arbitrary shape has raised great interest recently, being studied both theoretically and experimentally (see e.g. Refs. [1,2] and references therein), especially in nanostructures or in mesoscopic systems smaller than 10 nm. In these systems the tunnelling time will eventually play an important role in determining transport properties, for example in the frequency-dependent conductivity response of mesoscopic conductors [3] and in the phenomenon of an adiabatic charge transport [4,5].

In most approaches to the tunnelling time problem, only the scattering configuration is considered, where the free electron (or wavepacket) comes from

the left (right) of a one-dimensional (1D) arbitrary potential barrier. More than one tunnelling-time component is involved in this time problem, regardless of whether we deal with the so-called Büttiker–Landauer (BL) τ^{BL} [6] or complex τ characteristic times (note that $|\tau| = \tau^{\text{BL}}$) [7,8]. Furthermore, this does not seem to be a peculiarity of quantum mechanical waves, but a general result, as the characteristic time associated with a classical electromagnetic wave is also a complex magnitude [9] and the two components of this magnitude are not entirely independent quantities, but are connected by Kramers–Kronig relations [10].

On the other hand, it is clear that there are other similar situations of practical interest that should be discussed in the same context of two time components, as was done for the scattering problem. One of these situations is the escape of an electron from localized states in a quantum well with one or sev-

* Corresponding author. E-mail: vgaspar@quijote.ugto.mx

eral surrounding barriers. The escape of an electron from a localized state in a quantum well connected to a continuum by a small barrier only on one side (Fig. 1a) can be found, for instance, in miniaturized metal-oxide-semiconductor transistors, in which electrons arrive at the quantized accumulation or inversion layers after scattering and can subsequently tunnel to the metal gate through a very narrow oxide layer that acts as the barrier [11]. Physically, this implies that the particles entering the quantum well region remain there for some time before being allowed to escape outside. Tunnelling escape time has also been studied by transient-capacitance spectroscopy [12], where electrically injected electrons undergo an escape process out of the quantum well, such as in a three-barrier, two-well heterostructure [13].

In the present work the tunnelling escape time with the local Larmor clock approach is reconsidered and an analytical expression for the escape time of an electron from a finite 1D disordered region is derived in terms of partial scattering matrix elements. We show that the coordinate dependent escape time (CDET) from the quantum well has two components, both a precession and a rotation time scales. We investigated a particular example of a

potential (schematically shown in Fig. 1b) and explicitly calculated the two components of the escape time, using the squared wavefunction in the well as the weight function.

Before proceeding, we should remark that a magnitude similar to the CDET, a set of local partial density of states (DOS) $dn_{\alpha\beta}(y)/dE$ and a set of sensitivities $\eta_{\alpha\beta}(y)$, were introduced in Ref. [3] considering the response of the system to a small perturbation of the potential $V(y)$. It was shown that the $dn_{\alpha\beta}(y)/dE$ and $\eta_{\alpha\beta}(y)$ (the spin precession and rotation in the Larmor clock approach, respectively) are connected to the scattering matrix elements and are based on both a preselection and postselection of carriers, i.e., the carriers are grouped according to the asymptotic region from which they arrive (β) and according to the asymptotic region into which they are scattered (α). The decomposition of the local DOS on a next-higher level, based only on a preselection (termed an injectivity) or only on a postselection (called an emissivity) leads in the Larmor clock approach to a single spin precession [3,14]. For instance, the emissivity is the local DOS generated by carriers incident from the asymptotic region α regardless into which region the carriers are finally scattered.

Note that in the case of CDET, with the electron initially localized in the quantum well, the momentum acts like an additional channel index. This means that we can specify the incident channel and also the momentum sign (positive or negative) of the particles whose contribution to the local density of states we want to consider. This then leads to a local partial DOS and a sensitivity which, in addition to the usual channel indexes, also has a momentum index. The CDET is very sensitive to the initial position y_0 (at least it has a singularity in the quantum well, as discussed below). In order to obtain a result that is independent of the initial position of the electron, we averaged the different CDET inside the well by using an appropriate weighting function.

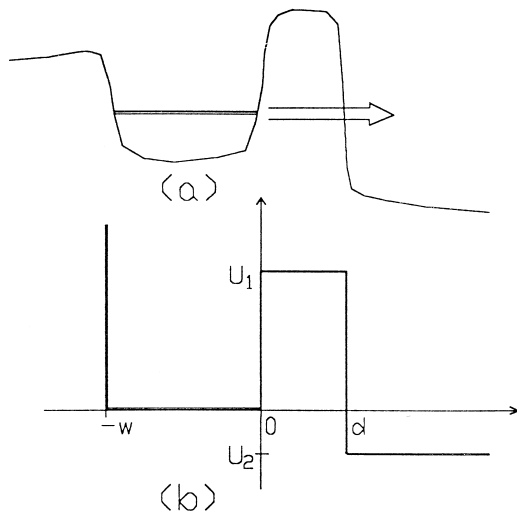


Fig. 1. Schematic representation of the quantum well connected to a continuum by a barrier on only one side. (a) General potential profile. (b) Simplified potential profile, with a hard wall condition at $-w$, used in this paper.

2. Lifetime calculation procedures

According to the general theory of quasistationary states [15], it is possible to reduce the time-depen-

dent Schrödinger equation to the time-independent ordinary differential equation only if we select a discrete complex value of energy \tilde{E} . The energy level of the particle state inside the well is connected with the real part of this complex energy, and the lifetime of this state is related to the imaginary part. Thus, the standard method for calculating the escape time is to expand the complex energy \tilde{E} in the immediate neighbourhood of any resonance energy level, e.g. E_1 , as $\tilde{E} = E_1 - i\Gamma/2$ ($\Gamma \ll E_1$), where Γ is the level width (the resonance width) connected with the lifetime by $\tau_{\text{LT}} = \Gamma^{-1}$. Moreover, as lifetime refers to the probability of an electron leaving the potential well per unit time, it is directly related to the electric current through the structure. To obtain the lifetime we can calculate the LDOS in the well and measure the width at half height of the peaks found at the quasibound levels. To do so, we can assume a wavefunction of fixed amplitude for $y > d$, solve the Schrödinger equation throughout the whole structure (see Fig. 1a) and evaluate $\text{LDOS} = \int_{-w}^0 |\psi(y)|^2 dy$ within the well. This procedure behaves well provided the peaks in the LDOS have a lorentzian-like shape, so that the width at half height can be accurately obtained. This approach also poses computational limitations for opaque barriers, in which the peaks are very narrow, as the step used in the energy sweep must be extremely small. In such a case it is better to use an approximate perturbative approach based on Bardeen's perturbation Hamiltonian [16]. First, we must obtain the unperturbed bound levels, E_1 , for an infinite-width barrier (Fig. 2a), that fulfil the following condition (we chose the parameters such that only a single bound state E_1 exists):

$$\sin(k_1 w) + \frac{k_1}{\gamma} \cos(k_1 w) = 0, \quad (1)$$

where $k_1 = \sqrt{E_1}$ and $\gamma = \sqrt{U_1 - E_1}$ ($\hbar = 2m = 1$, m is the electron free mass).

Second, the lifetime is obtained as follows:

$$\frac{1}{\tau_{\text{LT}}(E_1)} = W_{12}(E_1) \rho_2(E_1),$$

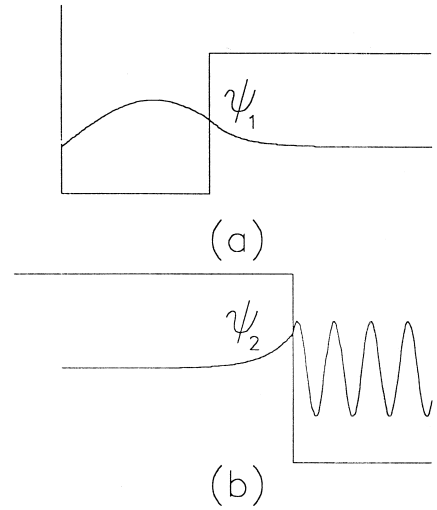


Fig. 2. Schematic representation of the simplified potential profiles used in the perturbative approach: (a) quantum-well with an infinite-width barrier; (E_1 is the single bound state defined in the text); (b) step profile used to obtain the wave function in the continuum.

where $\rho_2(E_1) = L/2\pi k_3$ is the density of states for $y > d$, and

$$W_{12} = 2\pi \left| \psi_1 \frac{d\psi_2}{dy} - \psi_2 \frac{d\psi_1}{dy} \right|^2.$$

$\psi_1(y)$ and $\psi_2(y)$ are the normalized wavefunctions obtained with the potential profiles shown in Fig. 2a and b, respectively, and L is a normalization length for $y > d$. The result is

$$\tau_{\text{LT}} = \frac{(1 + \gamma w)(1 + \beta^2)(1 + \xi^2)}{16 \cdot k_1^2 \cdot \xi} \exp(2\gamma d), \quad (2)$$

where $k_3 = \sqrt{E - U_2}$, $\beta = k_1/\gamma$, $\xi = \gamma/k_3$. A similar expression to Eq. (2) can be found, for sufficiently high and wide barriers, using also a scattering matrix approach (see e.g. [17]). But the validity conditions for these expressions are the same ones that make a calculation based on the LDOS difficult. That is to say, the narrower the resonance, the more valid the perturbative approach. It should be pointed out that the standard phase shift calculation (see Eq. (8) or Eq. (17)), also can identify and localize sharp

resonance in the limit of an opaque barrier, as it is plotted in Fig. 3b (solid line). But as we see the maximum of $\langle \tau_{y1}^{\text{esc}} \rangle$ does not coincide, with the τ_{LT} lifetime expression (2) at an energy very close to the bound level in the opaque barrier case. For this reason we use the above procedure as it provides a simple expression for an opaque barrier, and the error produced with respect to the LDOS procedure is very small for reasonably high values of the barrier strength, γd . For example, with a barrier height of $U_1 = 1$, the relative error for the ground level is less than 1% for $\gamma d > 1.7$, if $w = 5$ ($E_1 = 0.270$), while it is greater than 5% for $\gamma d < 2.6$, if $w = 2$ ($E_1 = 0.899$). The error is very small in important practical cases since, for example, even in

the narrowest oxide layers used in silicon devices, $\gamma d > 9$. However, in other materials with smaller barrier heights the error can be too high.

3. Local Larmor clock

The Larmor clock approach, based on an idea by Baz' et al. [17] to utilize the Larmor precession frequency of the spin produced by a weak magnetic field confined to the barrier and acting within the barrier region, leads us to the BL time τ^{BL} [6]. In this method, which is the most extensively studied, the spin is thought to be initially polarized perpendicular to the direction of the electron's motion (y direction). The rotation of the spin, as it traverses the barrier, is then studied by determining the time evolution of its z component along the magnetic field perpendicular to y , and along the y direction. Two times, τ_y^{BL} and τ_z^{BL} , are determined as the inverse expectation values of the y and z components, respectively, of the Larmor frequency. Büttiker's analysis of the Larmor clock has been extended to the 1D arbitrary barrier, using the surface GF method in Ref. [18]. The two characteristic times appearing in the magnetic clock approach were shown to correspond to the real and imaginary components of a single quantity, defined as an integral of the GF $G(y, y; E)$ for an open and finite 1D arbitrary system confined to the segment $0 \leq y \leq L$. The final result for the complex traversal time τ can be expressed in terms of partial derivatives with respect to energy E

$$\tau = \tau_z + i\tau_y = \int_0^L G(y, y; E) dy = \left\{ \frac{\partial \ln t}{\partial E} + \frac{r + r'}{4E} \right\} \quad (3)$$

where r and r' are the reflection amplitudes from the left and from the right, respectively. t is the transmission amplitude of the region considered and is independent of the incident direction.

The GF method was generalized to the electron escape problem from 1D disordered regions in [19], based on the local version of the Larmor clock [20]. It was shown that, in the case of a quantum well surrounded by right and left arbitrary barriers, and an

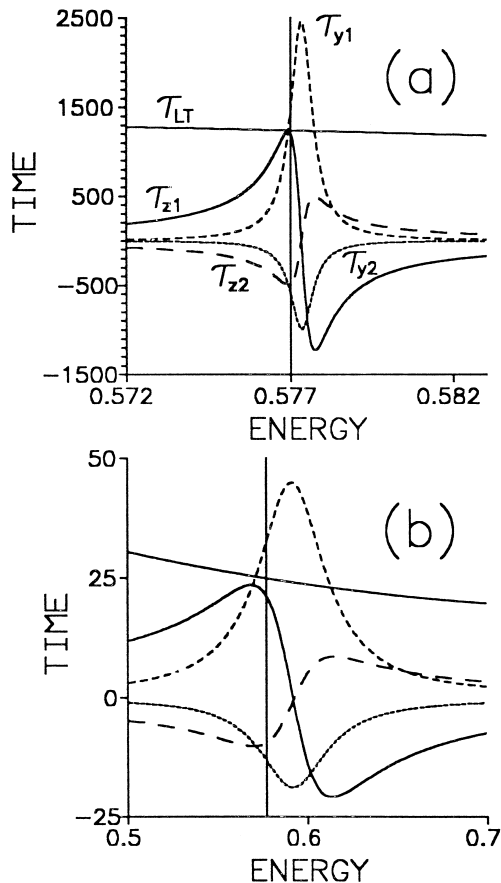


Fig. 3. The time components as a function of energy for the potential profile depicted in Fig. 1b, with $U_1 = 1$, $U_2 = -1$, and $w = 3$, for two different d values: (a) $d = 5$, and (b) $d = 2$. The different curves are labelled in (a).

additional weak magnetic field \mathbf{B} oriented in the z direction and finite only in the interval $[y_0, L]$, the right-hand side and the left-hand side CDET have two components, i.e. both a precession and rotation of spin. For instance, the right-hand side CDET $\tau_r^{\text{esc}}(y_0, L; E)$ is given by

$$\begin{aligned} \tau_r^{\text{esc}}(y_0, L; E) &= \tau_{r,z}^{\text{esc}} + i\tau_{r,y}^{\text{esc}} = \int_{y_0}^L G(y, y; E) dy \\ &= \left\{ \frac{\partial \ln t_r}{\partial E} + \frac{\tilde{r}_r + r'}{4E} \right. \\ &\quad \left. + \frac{1}{2}(1 - \tilde{r}_r) \frac{\partial}{\partial E} \ln \frac{1 - \tilde{r}_r}{1 + \tilde{r}_r} \right\}. \quad (4) \end{aligned}$$

Here, $t_r \equiv t_r(y_0, L; E)$ is the complex amplitude of transmission only through the right barrier and r' is the reflection amplitude of the electron from the whole system, when it falls in from the right (see Eq. (3)). $\tilde{r}_r \equiv \tilde{r}_r(y_0, L; E)$ has a slightly different meaning: the tilde mark signifies that the given quantity is calculated in the presence of the left and right barriers [19]. Thus, \tilde{r}_r is the complex amplitude of reflection from the right barrier in the presence of the left barrier, when the electron falls into this barrier from the left.

Note that the first term on the right-hand side of the above equations mainly contains information about the region of the barrier, while most of the information about the boundary is provided by the second and third terms. The integral in Eq. (4) runs from y_0 to L , instead of 0 to L as in the case of a free incident electron and obviously, for $y_0 = 0$, coincides with Eq. (3). For the special case of a rectangular barrier, the integral $\int_{y_0}^L G(y, y; E) dy$ leads us to the results of Ref. [20]. Analogous expressions hold for the particles escaping to the left-hand side of the disordered region.

We have thus arrived at a simple relationship between the two CDET components of an electron from a finite disordered region and the *local scattering-matrix elements*. Eq. (4) makes it evident that the time required by an electron to cover a distance L in the disordered region is extremely sensitive to the boundary conditions and to its initial position y_0 . We will see below that $\tau_{r,y}^{\text{esc}}(y_0, L; E)$ in a quantum well has a singularity at the initial position y_0 .

To obtain manageable analytical expressions for two time components of Eq. (4), we have applied

this formalism to the simplified structure depicted in Fig. 1b. A hard wall condition at $x = -w$ reduces the problem to escape to only one open channel: transmission to the right. Using standard methods of quantum mechanics it is easy to show that the straightforward calculations of the quantities in Eq. (4) lead to the result:

$$\begin{aligned} \tau_r^{\text{esc}}(y_0, L; E) &= \frac{d}{dE} \ln t_r(y_0) \\ &\quad - \frac{y_0}{2k_1 \sin k_1 y_0} \frac{A(y_0) + i\xi B(y_0)}{A + i\xi B} \\ &\quad + \frac{1}{4} \left\{ \frac{A - i\xi B}{A + i\xi B} \frac{1}{k_3^2} \right. \\ &\quad \left. - \frac{1}{k_1^2} \left[1 - 2 \frac{A(y_0) + i\xi B(y_0)}{A + i\xi B} \right] \right\} \\ &\quad \times \cos k_1 y_0 \Bigg\}, \quad (5) \end{aligned}$$

where w , d , U_1 and U_2 are defined in Fig. 1b, and

$$t_r(y_0) = 2\sqrt{\frac{k_1}{k_3}} \frac{\sin k_1 y_0}{A + i\xi B} \quad (6)$$

$$A = \sin k_1 w \cosh \gamma d + \beta \cos k_1 w \sinh \gamma d$$

$$B = \sin k_1 w \sinh \gamma d + \beta \cos k_1 w \cosh \gamma d$$

$$A(y_0) = \sin k_1(w - y_0) \cosh \gamma d \\ + \beta \cos k_1(w - y_0) \sinh \gamma d$$

$$B(y_0) = \sin k_1(w - y_0) \sinh \gamma d \\ + \beta \cos k_1(w - y_0) \cosh \gamma d.$$

By writing

$$t_r(y_0) = [T_r(y_0)]^{1/2} e^{i\varphi}$$

we obtain for Re and Im parts of the first term on the right-hand side of Eq. (5), i.e., for $d \ln t_r(y_0)/dE$ the following expressions ($G \equiv A^2 + \xi^2 B^2$):

$$\begin{aligned} \tau_{z1}^{\text{esc}} &= \frac{1}{2} \frac{d \ln T_r(y_0)}{dE} = \frac{1}{2k_1} \frac{y_0}{\tan(k_1 y_0)} \\ &\quad + \frac{1}{2} \frac{d}{dE} \left[\beta \cdot \xi \cdot G^{-1} \right], \quad (7) \end{aligned}$$

$$\tau_{y1}^{\text{esc}} = \frac{d\varphi}{dE} = - \frac{d}{dE} \tan^{-1} \left(\frac{\xi B}{A} \right). \quad (8)$$

As for the Re and Im parts of the second and third terms of Eq. (5), noted below as $\langle \tau_{z2}^{\text{esc}} \rangle$ and $\langle \tau_{y2}^{\text{esc}} \rangle$ respectively, we will only write averaged expressions (see Eq. (12) and (13)).

Note that the first term in τ_{z1}^{esc} contains a divergence. In order to avoid divergences in calculating τ_r^{esc} , and to obtain a result independent of the initial position of the electron, we will average the different time components by using the squared wavefunction in the well as the weight function, according to

$$\langle \tau_r^{\text{esc}} \rangle = \frac{\int_0^w \tau \sin^2 k_1 y_0 dy_0}{\int_0^w \sin^2 k_1 y_0 dy_0}. \quad (9)$$

The resulting averaged time components are

$$\langle \tau_{z1}^{\text{esc}} \rangle = \frac{1}{4k_1^2} \frac{\sin(2k_1 w) - 2k_1 w \cos(2k_1 w)}{2k_1 w - \sin(2k_1 w)} + \frac{1}{2} \frac{d}{dE} [\beta \cdot \xi \cdot G^{-1}] \quad (10)$$

$$\langle \tau_{y1}^{\text{esc}} \rangle = \tau_{y1}^{\text{esc}} \quad (11)$$

$$\langle \tau_{z2}^{\text{esc}} \rangle = -\frac{F_1}{4k_1^2} + G^{-1} \left\{ \frac{1}{4k_3^2} (A^2 - \xi^2 B^2) + \frac{F_2}{4k_1^2} (AC + \xi^2 BD) \right\} \quad (12)$$

$$\langle \tau_{y2}^{\text{esc}} \rangle = \xi G^{-1} \left\{ \frac{-2AB}{4k_3^2} + \frac{F_2}{4k_1^2} (AD - BC) \right\}, \quad (13)$$

with

$$F_1 = k_1 w - \frac{1}{4} \frac{\sin(4k_1 w) - \sin(2k_1 w) + 2k_1 w \cos(2k_1 w)}{2k_1 w - \sin(2k_1 w)} \quad (14)$$

$$F_2 = k_1 w - \sin(k_1 w) \cos(k_1 w) \quad (15)$$

and

$$C = \cos k_1 w \cosh \gamma d - \beta \sin k_1 w \sinh \gamma d$$

$$D = \cos k_1 w \sinh \gamma d - \beta \sin k_1 w \cosh \gamma d.$$

Note that the first term in $\langle \tau_{z1} \rangle$, which corresponds to the initial position of the electron, cancels out with

the two last terms in F_1 . Nevertheless, we will keep these terms since we are interested in studying the four time components separately.

For further discussion of the results in detail, let us write explicit expressions for $\langle \tau_{z1}^{\text{esc}} \rangle$ and $\langle \tau_{y1}^{\text{esc}} \rangle$ in the limit of an opaque barrier ($\gamma d \gg 1$) and near the resonance (see Eq. (1)). Since the large contributions to the $\langle \tau_{z1}^{\text{esc}} \rangle$ near the resonance come from the second term, we approximately have from Eq. (10)

$$\langle \tau_{z1}^{\text{esc}} \rangle = \frac{(1 + \gamma w)(1 + \beta^2)(1 - \xi^2)}{4k_1^2(1 + \xi^2)} \exp(2\gamma d). \quad (16)$$

The expression for $\langle \tau_{y1}^{\text{esc}} \rangle$ is

$$\langle \tau_{y1}^{\text{esc}} \rangle = \frac{\xi(1 + \gamma w)(1 + \beta^2)}{2k_1^2(1 + \xi^2)} \exp(2\gamma d). \quad (17)$$

We have thus arrived for the tunnelling escape time of an electron from a localized state in quantum well at two expressions. Comparison of these two components, i.e. Eq. (16) and Eq. (17) with the lifetime expression (2) will be done in the next section (see Fig. 3). Note that the curves as a function of energy corresponding to Eq. (16) and (17) are very similar and show a sharp resonance in the immediate neighbourhood of the ground energy level. The only major difference between these two time components is the shift and magnitude of the maxims.

It is easy to check from Eqs. (2), (16) and (17) that at the specific energy $E = (U_1 + U_2)/2$ ($\xi = 1$), we have $\langle \tau_{z1}^{\text{esc}} \rangle = 0$ and $\langle \tau_{y1}^{\text{esc}} \rangle = 2\tau_{\text{LT}}$, i.e. the phase time is twice as long as the lifetime of the electron.

Concluding this section, note that the conservation of angular momentum, similar to the case of the scattering process, also holds in the case of one open channel:

$$T_{r,z}^{\text{esc}} + \tilde{R} \tilde{\tau}_{r,z}^{\text{esc}} = 0, \quad (18)$$

where $\tilde{R} = \tilde{r}r^*$ is the coefficient of reflection from the right barrier in the presence of the left barrier, when the electron falls into this barrier from the left (see Eq. (4)). $\tilde{\tau}_{r,z}^{\text{esc}}$ is the reflection time from the same right barrier (an explicit expression will be given elsewhere).

This result indicates that summing the positive and negative momentum index for the escaping elec-

trons leads us to the results in Ref. [14], where it was shown that for a single contact there is no spin rotation. In terms of the sensitivities $\eta_{\alpha\beta}(y)$, mentioned in the Introduction, this means that $\eta_{21}(y) + \eta_{11}(y) = 0$.

4. Results

At this point, let us examine the relationship between the five time components we have defined: the four components of the complex time (see Eqs. (10)–(13)) and the lifetime (2). This comparison is shown in Fig. 3 for the following parameter values: $U_1 = 1$, $U_2 = -1$, $w = 3$, for two d values ($d = 5$ in Fig. 3a, and $d = 2$ in Fig. 3b). An opaque barrier has been chosen in Fig. 3a to ensure the accuracy of the lifetime expression, but in Fig. 3b the estimated relative error for the lifetime expression is about 16%. The vertical line corresponds to the ground energy level when the barrier width is infinite. The modulus of the total time is plotted in Fig. 4 in the two cases. The following conclusions can be drawn from these figures:

(a) The two real parts of the complex time have a similar shape but opposite signs. The same applies to the two imaginary parts. So, the resulting real and imaginary times are lower than those predicted by only the transmission coefficient.

(b) The maximum of component $\langle \tau_{z1}^{\text{esc}} \rangle$ coincides with the lifetime expression at an energy very close

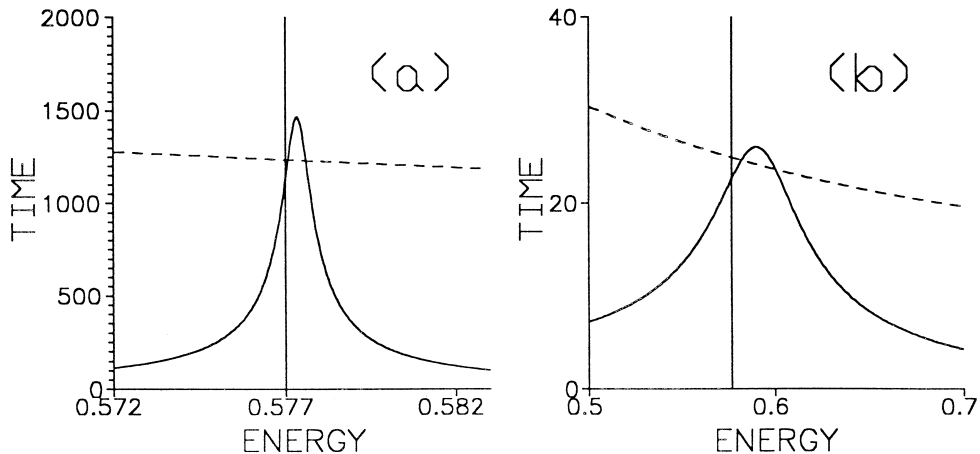


Fig. 4. Modulus of the total time (full line) for the two cases represented in Fig. 3. The vertical line corresponds to the ground energy level when the barrier width is infinite.

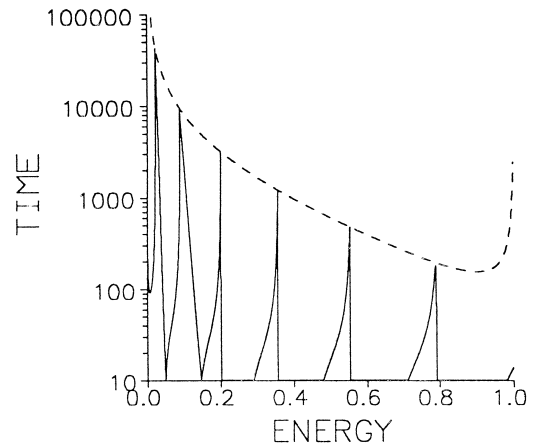


Fig. 5. Comparison between τ_{z1}^{esc} (solid line) and lifetime (dashed line) in a case with $d = 3$ and $w = 20$, so that several quasibound levels are found with energies lower than the barrier maximum.

to the bound level in the opaque barrier case (Fig. 3a). With the narrow barrier (Fig. 3b) both results deviate, but in this case the lifetime expression overestimates the lifetime by about 16% while the maximum of component $\langle \tau_{z1}^{\text{esc}} \rangle$ still provides an accurate value. Furthermore, this maximum is produced at an energy lower than the bound level, as predicted by the first-order perturbation theory.

(c) The maximum of the total tunnelling-time modulus is slightly higher than the lifetime, but the values of this total time modulus at the bound-level energy, which is where lifetime is calculated, are slightly lower than the lifetime.

Obtaining the lifetime through the maximum of a magnitude is useful, as it is computationally easier to detect a maximum than a width at half height. Fig. 5 shows a comparison between $\langle \tau_{z1}^{\text{esc}} \rangle$ (solid line) and the lifetime (dashed line) in a case with $d = 3$ and $w = 20$, so that there are several quasibound levels with energies lower than the barrier maximum. As shown, a good agreement is found between the two magnitudes.

To conclude, we have shown that the escape time of an electron from quantum well is a complex quantity. The $\tau_z^{\text{esc}}(y_0; E)$ component, even in the case of escaping through only one open channel, always exists. In the case of a potential well with a hard wall condition on one side this time component, exactly coincides with the lifetime expression obtained with a different approach. The standard phase shift calculation, i.e. the $\tau_y^{\text{esc}}(y_0; E)$ component of the escaping time, in the same limit of an opaque barrier leads us to the relatively big error. Note that in this paper coincidence of the $\langle \tau_{z1}^{\text{esc}} \rangle$ with the lifetime expression (2) was only checked analytically for the simplified structure depicted in Fig. 1b, but it should be clear that the concepts discussed in this article apply also for more complicated cases and thus the maximum of $\langle \tau_{z1}^{\text{esc}} \rangle$ provides the lifetime for any potential shape.

Acknowledgements

We would like to thank B. Altshuler and M. Büttiker for very useful discussions and a critical reading of the manuscript. J.A.L.V. would like to acknowledge the Spanish Dirección General de Enseñanza Superior e Investigación Científica for financial support under contract No. PB97-0815. V.G.

would like to thank the CONACyT (Catedra Patronal de Excelencia Nivel II) for financial support.

References

- [1] R. Landauer, Th. Martin, *Rev. Mod. Phys.* 66 (1994) .
- [2] V. Gasparian, M. Ortuño, G. Schön, U. Simon, Tunneling time in nanostructures, review chapter, in: H.S. Nalwa (Ed.), *Handbook of Nanostructured Materials and Nanotechnology*, Vol. 2, Chap. 11, Academic Press, San Diego, 1999, pp. 513–569.
- [3] M. Büttiker, H. Thomas, A. Pretre, *Z. Phys. B* 49 (1994) 133.
- [4] P.W. Brouwer, *Phys. Rev. B* 48 (1998) R10135.
- [5] F. Zhou, B. Spivak, B. Altshuler, *Phys. Rev. Lett.* 82 (1999) 608.
- [6] M. Büttiker, *Phys. Rev. B* 27 (1983) 6178.
- [7] D. Sokolovski, L.M. Baskin, *Phys. Rev. A* 36 (1987) 4604.
- [8] C.R. Leavens, G.C. Aers, *Solid State Commun.* 63 (1987) 1101.
- [9] V. Gasparian, M. Ortuño, J. Ruiz, E. Cuevas, *Phys. Rev. Lett.* 75 (1995) 2312.
- [10] V. Gasparian, G. Schön, M. Ortuño, J. Ruiz, *Ann. Phys.* 7 (1999) 756.
- [11] F. Rana, S. Tiwary, D.A. Buchanan, *Appl. Phys. Lett.* 69 (1996) 1104.
- [12] E. Martinet, E. Rosencher, F. Chevoir, J. Nagle, P. Bois, *Phys. Rev. B* 44 (1991) 3157.
- [13] H.-Z. Zheng et al., *Phys. Rev. B* 51 (1995) 11128.
- [14] V. Gasparian, T. Christen, M. Büttiker, *Phys. Rev. A* 54 (1996) 4022.
- [15] L.D. Landau, E.M. Lifshitz, *Quantum Mechanics*, Pergamon, New York, 1982.
- [16] J. Bardeen, *Phys. Rev. Lett.* 6 (1961) 57.
- [17] I.A. Baz', Ya.B. Zel'dovich, A.M. Perelomov, *Scattering, Reactions and Decay in Nonrelativistic Quantum Mechanics*, Wiener Bindery, Jerusalem, 1969.
- [18] V. Gasparian, M. Pollak, *Phys. Rev. B* 47 (1993) 2038.
- [19] V. Gasparian, *Superlattices and Microstructures* 23 (1998) 809.
- [20] C.R. Leavens, G.C. Aers, *Solid State Commun.* 67 (1988) 1135.